UNITED STATES DEPARTMENT OF THE INTERIOR

GEOLOGICAL SURVEY

FLUID IMPACT CRATERS AND HYPERVELOCITY--HIGH VELOCITY IMPACT EXPERIMENTS IN METALS AND ROCKS

by

H. J. Moore, D. E. Gault, and

R. W. MacCormack

November 1962

Open File Report

This report concerns work done on behalf of the

National Aeronautics and Space Administration

UNITED STATES DEPARTMENT OF THE INTERIOR

GEOLOGICAL SURVEY

FLUID IMPACT CRATERS AND HYPERVELOCITY--HIGH VELOCITY IMPACT EXPERIMENTS IN METALS AND ROCKS

by

H. J. Moore, D. E. Gault[1/], and

R. W. MacCormack[1/]

November 1962

Open File Report

This report concerns work done on behalf of the National Aeronautics and Space Administration

This preliminary report is released without editorial and technical review for conformity with official standards and nomenclature.

1/ Ames Research Center, National Aeronautics and Space Administration, Moffett Field, California.

Contents

Illustrations

Table

N64-22459

Fluid impact craters and hypervelocity--high velocity impact experiments in metals and rocks

By H. J. Moore, D. E, Gault[1/], and
R. W. MacCormack[1/]

Abstract

The effective deformation strength for a hemispherical water crater is equal to the sum of strength due to hydrostatic pressure head, the strength due to surface tension and the estimated viscous head loss, as shown in the following equation:

$$S_w = \frac{3}{8}\rho g p + \frac{3\gamma}{p} + \mu \frac{1}{t}\int_0^t \frac{\frac{d(z)}{dt}}{\frac{Vol_p}{\pi p^2}} dt,$$

where: ρ is the density of water, g is the acceleration of gravity, p is the maximum crater depth, γ is the surface tension of water, μ is the viscosity of water, t is the duration of the cratering event, $\frac{d(z)}{dt}$ is the radial velocity of the fluid shell, and Vol_p is the volume of the projectile. Deformation strengths of water which are computed in this manner are in substantial agreement with calculations of deformation strengths using a formula derived on a theoretical basis by Charters and Summers for impact craters formed in metal targets in the fluid-impact regime.

Fluid-impact or near-fluid-impact craters in metals and rocks may be correlated with fluid-impact craters produced by water drops impacting

---

1/ National Aeronautics and Space Administration, Ames Research Center, Moffett Field, California.

with water when the deformation strength of rocks and metals are related to the shear or compressive strengths of the target materials. Although the correlation using strengths at low confining pressures is not in perfect accord with theory, the use of the product of the heat of fusion and density of the target material as a maximum possible deformation strength suggests that the effective deformation strength for rocks and metals during impact lies between the unconfined compressive strength and the product of the heat of fusion and density of the target material. The use of shear strengths and densities of the target at 49-kilobars confining pressure improves the correlation between craters produced in metals near the fluid-impact regime, the theory of Charters and Summers, and craters produced by water drops impacting water. Craters in rock do not correlate exactly with water craters and metal craters when the target shear strengths and densities at 49-kilobars are used, but such a difference should be expected.

It is concluded that shear or compressive strengths of the target material are more realistic parameters to use in correlating impact-crater data than acoustic velocities.

Introduction

The impact phenomena of hypervelocity and high-velocity projectiles with rock and metal targets are being studied in a cooperative research program, by the U.S. Geological Survey and the Ames Research Center of the National Aeronautics and Space Administration. This paper deals with the comparison of: (a) fluid-impact craters produced by water drops impacting water, (b) hypervelocity and high-velocity impact craters produced by impact of steel, aluminum, and polyethylene projectiles with basalt, and (c) hypervelocity and high-velocity impact craters in metals.

The theoretical formula of Charters and Summers (1959) is tested in this investigation. The formula, as tested, is approximately valid for impact of water drops into water. In addition, the formula demonstrates that deformation strengths of metals and rocks are placed at some value between a maximum possible deformation strength of the target material and its compressive strength at low confining pressures. The maximum deformation strength is represented by the product of the heat of fusion and density of the target material. The use of shear strengths and densities of the metal and rock-target materials at 49 kilobars for parameters yields fair agreement between (a) craters produced by water drops impacting water, (b) the theory of Charters and Summers, and (c) hypervelocity impact experiments in and near the fluid-impact regime using rock and metal targets.

It is concluded that shear or compressive strengths of the target material are more realistic parameters than acoustic velocities, because water-drop cratering experiments cannot be correlated with theory or high- to hypervelocity impact-cratering experiments in rocks and metals when acoustic velocity is used as a parameter.

Cratering theory of Charters and Summers

A quantitative theory for craters produced by projectile impact in the fluid-impact regime has been proposed by Charters and Summers (1959). In their theory, the momentum of a uniformly expanding hemispherical shell composed of both the projectile and the target material is assumed to be equal to the projectile momentum by analogy with the ballistic pendulum:

$$m_{fs}\mu_{fs} = m_p V_p, \tag{1}$$

where

m_{fs} = mass of fluid shell,

μ_{fs} = velocity of fluid shell,

m_p = mass of projectile,

V_p = velocity of projectile.

The kinetic energy of the projectile is then compared to the kinetic energy of the fluid shell using the hydraulic analogy of the shaped charge penetration for which

$$\mu_{fs} = \frac{1}{2} V_p, \tag{2}$$

then

$$m_{fs}\mu_{fs}^2 = \frac{1}{2} m_p V_p^2. \tag{3}$$

The kinetic energy of the fluid shell is assumed to be used in the work of deformation in forming the crater:

$$\frac{1}{2} m_{fs}\mu_{fs}^2 = \int_0^p S\, 2\pi r^2 dr, \tag{4}$$

where

S = the deformation strength,

p = the maximum crater depth,

r = the radius of the hemispherical crater cavity.

Integration, when S is constant, gives

$$\frac{1}{2} m_{fs} \mu_{fs}^2 = \frac{2}{3} \pi p^3 S, \tag{5}$$

and since

$$m_{fs} \mu_{fs}^2 = \frac{1}{2} m_p V_p^2, \tag{6}$$

then

$$m_p V_p^2 = \frac{8}{3} \pi p^3 S, \tag{7}$$

or

$$S = \frac{3 m_p V_p^2}{8 \pi p^3}. \tag{8}$$

Then, taking into account experimental data and rearranging terms, the penetration formula becomes

$$\frac{p}{d} = \frac{1}{2} \left(\frac{\rho_p}{\rho_t} \right)^{1/3} \left(\frac{\rho_p V_p^2}{2S} \right)^{1/3}, \tag{9}$$

which can be rewritten

$$S = \frac{1}{16} \frac{\rho_p^2}{\rho_t} \frac{V_p^2}{\left(\frac{p}{d}\right)^3}.$$

where

d = diameter of the projectile,

ρ_p = density of the projectile,

ρ_t = density of the target.

Dr. Engel's water craters

Preliminary studies of craters produced by water drops impacting water (Engel, 1961) yield data that permits a quantitative test of the fluid-impact theory of Charters and Summers. The water-drop experiments employed projectiles of 11 mg, 56 mg, and 183 mg which impacted water with velocities of 400 to 700 cm/sec. The experiments of Engel produced temporary craters from 7.25 mm to 21.9 mm in depth. In addition, Engel points out many similarities between the water-drop experiments and some hypervelocity impact experiments.

Deformation strengths of the water for each experiment can be calculated in two ways: (1) by employing a knowledge of the physical properties of water and the experimental measurements and (2) by employing the theory of Charters and Summers.

Three types of resistance oppose the process of crater formation in water: (1) the hydrostatic pressure head, (2) surface tension, and (3) the resistance of the water to flow (or viscosity). The deformation strength then becomes

$$S_w = f(\rho_w g z) + f\left(\frac{2\gamma}{z}\right) + f\left(\frac{V_t \mu}{x}\right), \qquad (10)$$

where

S_w = deformation strength of water,

ρ_w = density of water,

g = acceleration of gravity,

z = a depth or vertical coordinate,

$\frac{V_t}{x}$ = a velocity gradient,

μ = viscosity of water (10^{-2} dynes-sec/cm^2),

γ = surface tension of water (72 dynes/cm).

During the cratering process in water the deformation strength related to the hydrostatic pressure head increases from zero to some finite value since z increases from zero to p or the maximum crater depth. The effective deformation strength resulting from the hydrostatic pressure head may be obtained by computing the work required to form a crater against the hydrostatic pressure head and relating this to the final crater volume. The work required to form a hemispherical crater against the hydrostatic pressure head may be expressed

$$W_{hh} = \int_0^F dF\ z = \int_0^{Vol} \rho_w g\ d(Vol)z, \qquad (11)$$

where

W_{hh} = work expended in overcoming hydrostatic pressure head,

dF = incremental force on an incremental volume of water removed from crater to surface of water,

p = maximum crater depth of hemispherical crater,

ρ_w = density of water,

g = acceleration of gravity,

z = depth or vertical coordinate,

d(Vol)= an incremental volume of water removed from crater to surface of water.

Integration of equation (11) yields

$$W_{hh} = \frac{\pi \rho g p^4}{4}. \qquad (12)$$

If the mean or effective deformation strength due to the hydrostatic pressure head is defined by S_{hh}, then

$$W_{hh} = S_{hh} \int_0^p 2\pi r^2 dr, \tag{13}$$

and

$$S_{hh} = \frac{3\rho_w g p}{8}. \tag{14}$$

The mean or effective deformation strength due to surface tension may be derived in a similar manner. The work required to overcome surface tension is

$$W_{st} = \int_0^{2\pi p^2} \gamma \, dA, \tag{15}$$

where

W_{st} = work expended in overcoming surface tension,

γ = surface tension of water,

dA = the change in area,

p = maximum crater depth of hemispherical crater,

then

$$W_{st} = 2\pi \gamma p^2, \tag{16}$$

and

$$W_{st} = S_{st} \int_0^p 2\pi r^2 \, dr, \tag{17}$$

where

S_{st} = effective or mean deformation strength due to surface tension,

or

$$S_{st} = \frac{3\gamma}{p}. \tag{18}$$

Approximate values for the deformation strength of the water due to viscosity during the cratering process may be obtained by assuming that the flow of the projectile and target material occurs near the projectile-target interface. The flow would occur within a layer having an effective thickness equal to twice the thickness of the projectile smeared evenly over a hemispherical crater at maximum depth. Also, it may be assumed

that the average velocities of the flow are approximately equal to the average radial velocities of the fluid shell. The estimated deformation strength due to viscosity then becomes

$$S_\mu = f\left(\frac{V_t}{x}\mu\right) = \mu \frac{1}{t} \int_0^t \frac{\frac{d(z)}{dt}}{\frac{2vol_p}{2\pi p^2}} dt, \qquad (19)$$

where

S_μ = deformation strength due to viscosity,

μ = viscosity of water $\left(\frac{10^{-2}\text{dynes-sec}}{\text{cm}^2}\right)$,

t = duration of cratering event,

$\frac{d(z)}{dt}$ = radial velocity of fluid shell,

vol_p = volume of projectile,

p = maximum crater depth

$\frac{V_t}{x}$ = velocity gradient.

The calculated deformation strengths for the individual experiments of water impacting water (Engel, 1961) using the effective deformation strengths due to hydrostatic pressure head, surface tension, and viscous head loss and assuming hemispherical craters are tabulated (table 1).

Deformation strengths for the water craters assuming spherical projectiles and hemispherical craters have been calculated using the Charters-Summers theory (equation 9). These deformation strengths are listed in table 1, column 5. In addition, the data are plotted in figure 1, where p is the maximum crater depth.

The assumption of hemispherical water craters which are actually prolate hemi-spheroids leads to minor errors, so that the calculations represent approximate values for the mean or effective deformation

strength of the water craters. The calculations do give us a magnitude for the mean or effective deformation strength of the water during cratering and this magnitude is near $\frac{1 \times 10^3 \text{ dynes}}{\text{cm}^2}$.

Table 1. Computed deformation strengths of water for craters produced by impact of water drops into water.

Experiment (Engel 1961)	(1) Hydrostatic pressure head (Equation 14) $\frac{3}{8}\rho_w g p$ (dynes/cm^2)	(2) Surface tension (Equation 18) $\frac{3\gamma}{p}$ (dynes/cm^2)	(3) Estimated strength due to viscosity (Equation 19) $f\left(\frac{V_t}{x}\mu\right)$ (dynes/cm^2)	(4) Total deformation strength (Equation 10) S_w (dynes/cm^2)	(5) Deformation strength calculated with Charters-Summers theory (Equation 9) $\frac{1}{16}\frac{\rho_p^a}{\rho_t}\frac{V^2}{(p/d)^3}$ (dynes/cm^2)
11-400	0.27×10^3	0.30×10^3	0.07×10^3	0.64×10^3	0.57×10^3
11-650	0.36×10^3	0.22×10^3	0.13×10^3	0.71×10^3	0.61×10^3
56-400	0.44×10^3	0.18×10^3	0.03×10^3	0.65×10^3	0.62×10^3
56-700	0.53×10^3	0.15×10^3	0.08×10^3	0.76×10^3	1.07×10^3
182-400	0.62×10^3	0.13×10^3	0.03×10^3	0.78×10^3	0.73×10^3
182-700	0.80×10^3	0.10×10^3	0.07×10^3	0.97×10^3	0.98×10^3

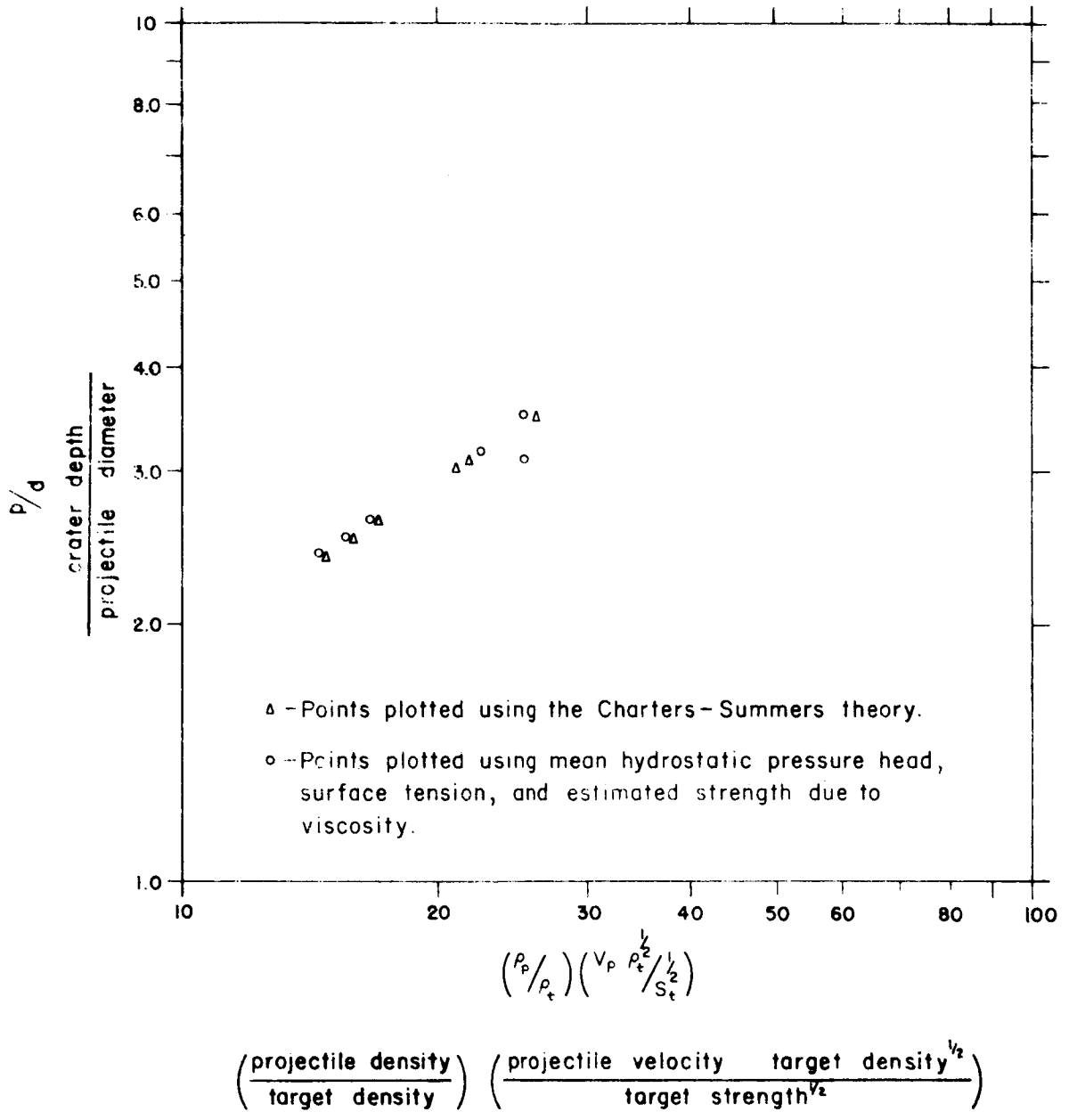

Figure 1. Graph comparing deformation strength of water computed by using the mean hydrostatic pressure head, surface tension and estimated strength due to viscosity, and the theory of Charters-Summers.

Parameters

Various parameters have been used to correlate hypervelocity fluid-impact experiments. The familiar empirical formula of Charters and Summers (1959) relates the experimental data on penetration to the projectile diameter, projectile density, target density, projectile velocity and the acoustic velocity of the target material:

$$\frac{p}{d} = 2.28 \left(\frac{\rho_p}{\rho_t}\right)^{2/3} \left(\frac{V}{c}\right)^{2/3}. \tag{20}$$

The acoustic velocity is then correlated with Young's modulus (E_t) of the target material:

$$C^2 = \frac{E_t}{\rho_t}. \tag{21}$$

In addition to the above parameters, the following may be used:

$$\frac{p}{d} = K \left(\frac{\rho_p}{\rho_t}\right)^{2/3} \left(\frac{V\rho_t^{1/2}}{S_t^{1/2}}\right)^{2/3}, \tag{22}$$

where

K = a constant,

S_t = deformation strength.

These parameters were selected primarily on the basis of equation 9. The term $\rho_t^{1/2}/S_t^{1/2}$ has the dimensions of time/distance and may be considered as the reciprocal of a velocity which is characteristic of the target material.

Experimental data using equation 22 for impact of metal projectile into metal, metal projectile into rock, and water projectile into water are shown in figure 2. In addition, a plot using the reciprocal of the square root of the heat of fusion in place of $\rho_t^{1/2}/S_t^{1/2}$ has been included in figure 2. This parameter, which has been suggested by Bromberg (in Palmer and others, 1960, p. 8), also has the dimensions of time/distance.

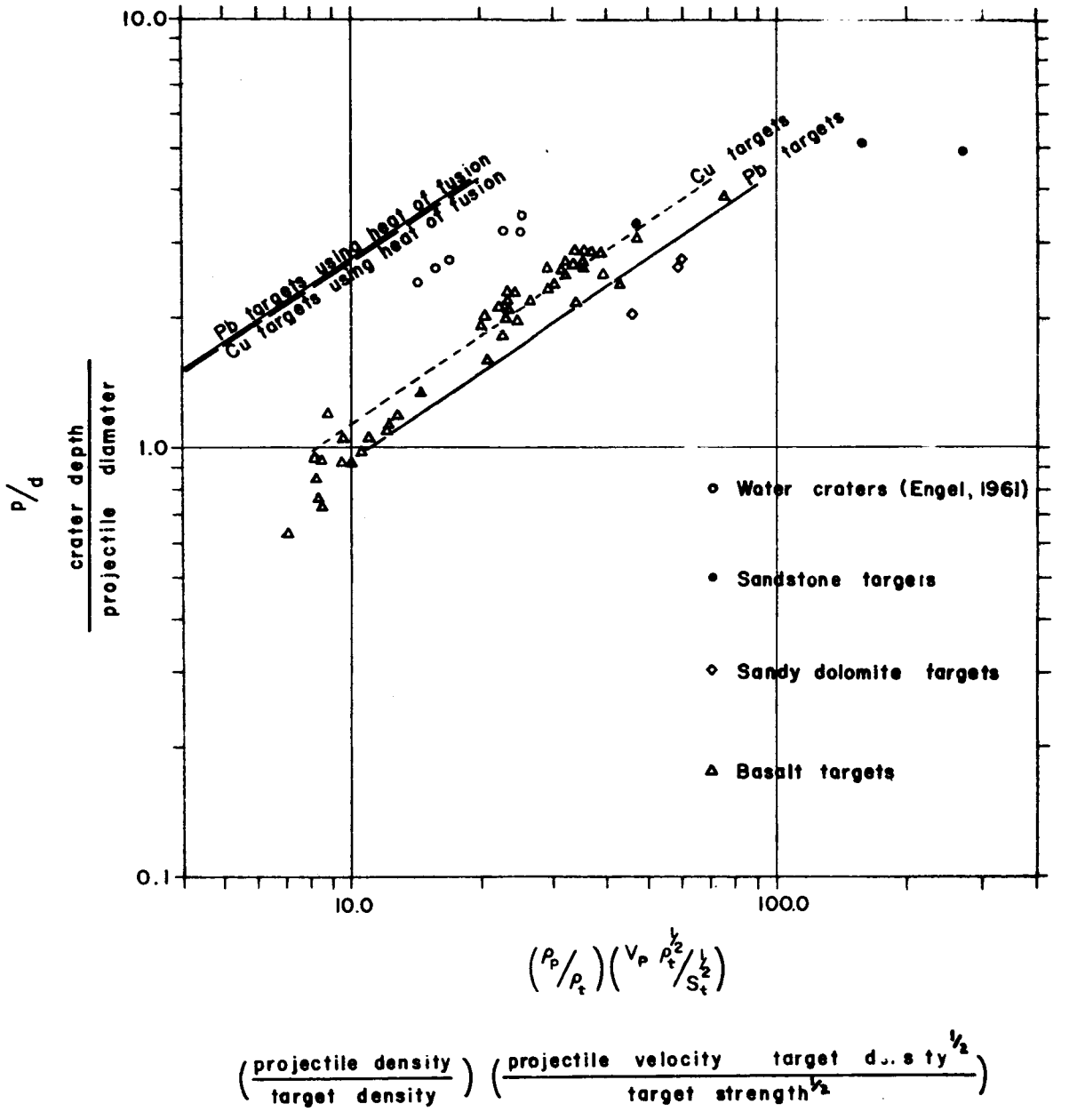

Figure 2. Graph comparing craters produced by impact of water drops into water, metal spheres impacting copper and lead targets, and metal and polyethylene spheres impacting rocks using $\rho_t^{\frac{1}{2}}/S_t^{\frac{1}{2}}$ as measured at normal confining pressures. A plot for copper and lead cratering experiments using the reciprocal of the square root of the target heat of fusion in place of $\rho_t^{\frac{1}{2}}/S_t^{\frac{1}{2}}$ is included.

Figure 2 is based on experimental data for impacts using rock targets, Moore and Gault (1962), Summers (1959), the Metals Handbook (Lyman, 1958, p. 905-909, 961-962), and actual determination of shear strengths of the rocks. The shear strengths used were as follows:

copper - 1.53×10^9 dynes/cm^2,

lead - 1.26×10^8 dynes/cm^2,

basalt - 8.6×10^8 dynes/cm^2,

sandy dolomite - 2.8×10^8 dynes/cm^2, and

sandstone - 1.9×10^8 dynes/cm^2.

A value for the heat of fusion of 2.12×10^9 ergs/gram was used for copper targets and 2.62×10^8 ergs/gram was used for lead targets.

If the sum of the mean hydrostatic pressure head, the mean surface tension factor, and the viscous head loss is considered to be analogous to compressive strength which is twice the shear strength for ideal plastic failure, the plot of the experimental data for metals and rocks would be moved toward the left by a factor of $\sqrt{2}$ when compressive strengths were used instead of shear strengths. Such a shift would reduce the difference between the experimental data for metals and rocks and the data for water.

The strength of rocks and metals with increasing confining pressure is not constant. More precise plotting of data would require a knowledge of the strength of the target material at elevated confining pressures because high confining pressures are produced during crater formation by impact of hypervelocity projectiles. If the maximum possible strength of the target is taken as the product of the heat of fusion and density of the target material, the deformation strength during cratering by hypervelocity and high velocity impacts would lie between the compressive strength at low confining pressures and the heat of fusion multiplied by the target density.

Strengths and densities at elevated confining pressures

Although considerable information about the density of some materials up to 700 kilobars confining pressure, and in some cases up to several megabars, is known (Rice and others, 1958, and Al'tshuler and others, 1960), little is known about the strength of materials above 49 kilobars. However, the existing data on the strengths and densities of metals and rocks may be used to illustrate how the parameter $\rho_t^{\frac{1}{2}}/S_t^{\frac{1}{2}}$ and the plot of cratering experiments in and near the fluid-impact regime might improve correlation of impact-cratering experiments.

The plots of hypervelocity-impact data for copper and lead in and near the fluid-impact regime indicate that $\rho_t^{\frac{1}{2}}/S_t^{\frac{1}{2}}$ is constant because of the constant slope of $\frac{2}{3}$ (Summers, 1959). If it is further assumed that $\rho_t^{\frac{1}{2}}/S_t^{\frac{1}{2}}$ for metals becomes constant at and above 49 kilobars and ρ_p/ρ_t is essentially constant, the shear strength and density at 49 kilobars (Bridgman, 1935, and Rice and others, 1958) may be used to evaluate $\rho_t^{\frac{1}{2}}/S_t^{\frac{1}{2}}$ at elevated pressures.

Justification for the assumption that ρ_p/ρ_t is constant may be obtained from compressibility data obtained with shock techniques. Compressibility ratios for copper, lead, aluminum, iron, and magnesium projectiles and copper and lead targets range between 0.850 and 1.065 at 100 kilobars and 0.850 and 1.175 at 500 kilobars. Thus the assumption of a constant ratio for ρ_p/ρ_t is valid within ±10 percent at 100 kilobars and ±16 percent at 500 kilobars and is within the scatter of experimental data for metals and rocks (see, for example, Charters and Summers, 1959, and Summers, 1959, p. 13). The shear strengths for lead and copper at 49 kilobars are 710 kg/cm^2 (6.96×10^8 dynes/cm^2) and 4700 kg/cm^2

(4.6×10^9 dynes/cm^2) (Bridgman, 1935). The densities of lead and copper which were obtained by extrapolation of densities obtained with shock-wave techniques (Rice and others, 1958) and static compression techniques (Bridgman, 1935) are 12.4 grams/cm^3 and 9.35 grams/cm^3 at 49 kilobars.

The use of the shear strengths and densities at 49 kilobars confining pressure [redacted] yields good results (compare fig. 3). In contrast with plots using shear strengths at low confining pressures, impact data for lead and copper are practically coincident. In addition, the agreement between fluid impacts produced by water drops into water and impact craters produced by metal projectiles into metal targets near the fluid-impact regime is improved.

Similar data are available for some rocks. In the case of basalt, no data are available for shear strengths at 49 kilobars. However, an extimate of 15.5×10^9 dynes/cm^2 for the strength of basalt at elevated confining pressures can be made using the shear strength of basalt glass, which is 17.0×10^9 dynes/cm^2, and pyroxenite, which is 14.0×10^9 dynes/cm^2 (Bridgman, in Robertson, 1955). Justification for this estimate is based on generalizations of shear strengths of rocks which tend to be approximately the same at elevated confining pressures (Robertson, 1955). The density of basalt at 49 kilobars may be estimated with data from shock-wave techniques (Lombard, 1961). Such an estimate yields 2.9 to 3.0 grams/cm^3.

The data plotted for basalt fall to the left of the metal and water craters (fig. 3). Such a difference should be expected because of the difference in the cratering process in metals and water and in rocks. This difference is due to the low tensile strength of rocks at low

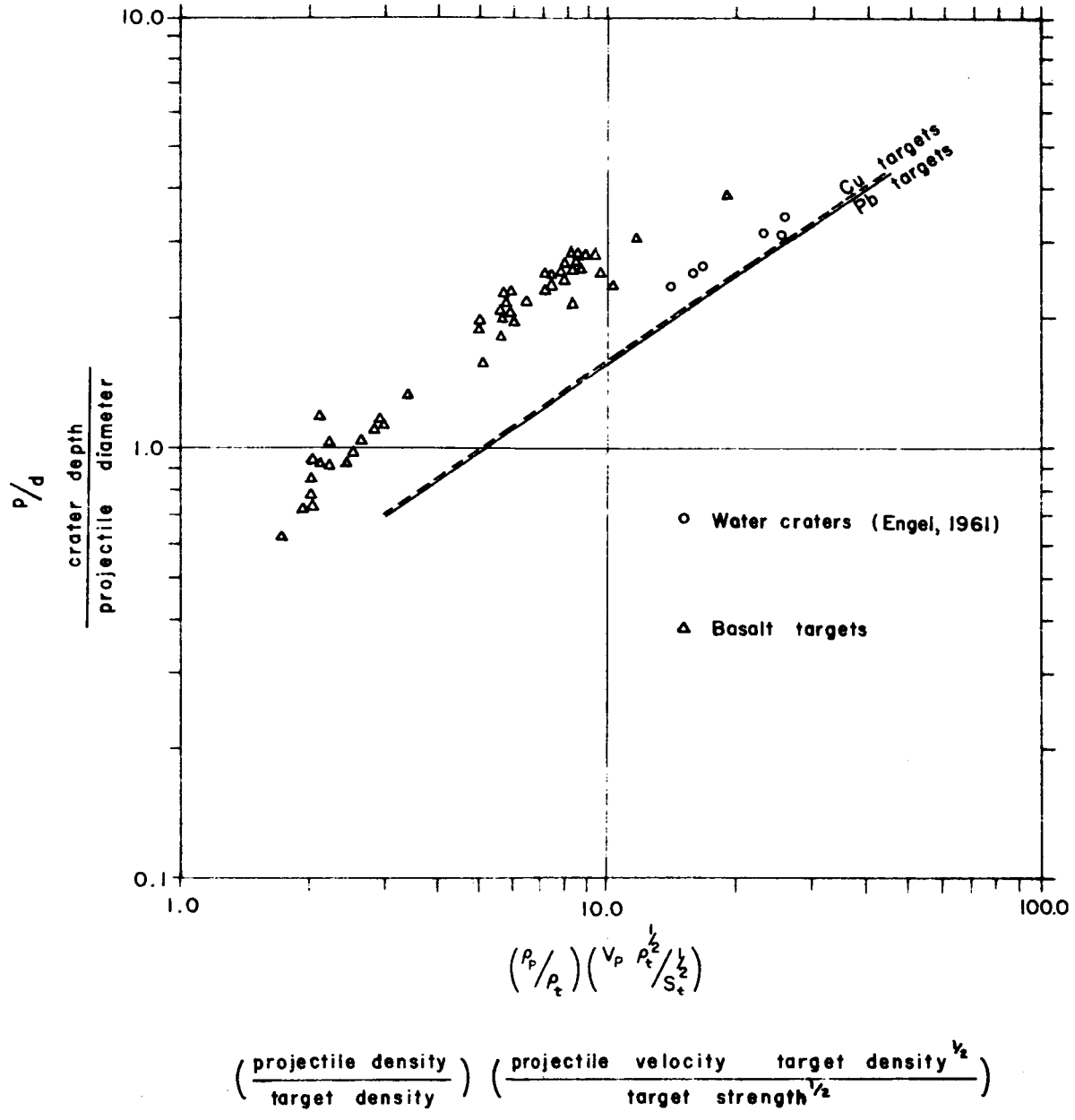

Figure 3. Graph comparing craters produced by impact of water drops into water, metal spheres impacting copper and lead targets, and metal and polyethylene spheres impacting basalt using $\rho_t^{\frac{1}{2}}/S_t^{\frac{1}{2}}$ as estimated for 49 kilobars confining pressure.

confining pressures. For craters of the scale of the laboratory experiments, the projectile is ejected completely from the crater along with rock debris, whereas in the case of metal craters the projectile smears out and plates the crater floor and walls (Summers, 1959). Plating also occurs in craters produced by water-drop impacts with water (Engel, 1961; Charters, 1960).

Proper appraisal and use of the parameters in equation 22 would require the knowledge of the average deformation strength of the target, the average density of the projectile, and the average density of the target during the cratering process.

Acoustic velocity as a parameter

The primary problem with acoustic velocity as a parameter is shown clearly in the case of fluid impacts of water into water. The use of the acoustic velocity of water (which is 1.5 km/sec) in Engel's experiments did not permit plotting of the fluid-impact water-drop experiments and the fluid-impact metal and rock experiments together in the same decade on log-log paper. In contrast, the use of either compressive strength at low or high confining pressure divided by the target density or the target heat of fusion permits such a plot.

Conclusions

1. The target strength is a more realistic parameter than the target acoustic velocity for correlation of data for hypervelocity impact craters in the fluid-impact regime and low-velocity hydrodynamic or fluid-impact craters. The partial success obtained when using target acoustic velocity is probably the result of a close correlation between strength and acoustic velocity for certain materials (see for example, Mauer and Rinehart, 1960), but the correlation does not hold for materials such as water.

2. The theory of Charters and Summers is approximately valid for fluid-impact craters produced by water drops impacting water and other impact craters in the fluid-impact regime.

3. Dynamic strengths of materials which yield under impact in the fluid-impact regime are greater than the strengths at low confining pressure but less than the product of the target density and heat of fusion when significant amounts of vaporization of the target do not occur.

4. The effects of target strength and target density at elevated confining pressures [redacted] for craters in rocks and metals produced in the fluid-impact regime can be semiquantitatively assessed using the existing data at 49 kilobars. Such data at 49 kilobars give fair agreement with theory, water-water impact, and reduces the discrepancy between lead and copper experimental data when shear strengths at low confining pressures are used.

5. Hypervelocity impact craters in rocks should be deeper than corresponding craters in metals and water in the fluid-impact regime

because the projectile is ejected along with debris in the case of rock, whereas plating of the projectile on the crater floors and walls occurs in metal and water craters.

6. More data on strengths at elevated confining pressures are needed in order to resolve the problem of the selection of parameters for correlation of hypervelocity impact data.

References cited

Al'tshuler, L. V., Kormer, S. B., Brazhnik, M. I., Vladimirov. L. A., Speranskaya, M. P., and Funtikov A. I., 1960, The isentropic compressibility of aluminum, copper, lead, and iron at high pressures: Soviet Physics JETP, v. 11, p. 766-775 (in English).

Bridgman, P. W., 1935, Effects of high shearing stress combined with high hydrostatic pressure: Phys. Rev., v. 48 p. 825-847.

Charters, A. C., 1960, High speed impact: Sci. Am., v. 203, no. 4 (Oct.), p. 128-140.

Charters, A. C., and Summers, J. L., 1959, Some comments on the phenomena of high-speed impact, in Decennial symposium, May 26, 1959, White Oak U.S. Naval Ordnance Laboratory, Silver Spring, p. 1-21.

Engel, O. G., May 1961, Collisions of liquid drops with liquids: Nat. Bur. Standards Tech. Note 89, 30 p.

Lombard, D. B., 1961, The hugoniot equation of state of rocks, in Fourth symposium on rock mechanics, March 30, 31, and April 1, 1961, Proceedings: Pennsylvania Mineral Industries Expt. Sta. Bull. No. 76, p. 143-152.

Lyman, Taylor, ed., 1958, Metals Handbook: Cleveland Ohio, The American Society for Metals, 4th repr., 1332 p.

Maurer, W. C., and Rinehart, J. S., 1960, Impact crater formation in rock: Jour. Appl. Physics, v. 31, p. 1247-1252.

Moore, H. J., and Gault, D. E., 1962, Current tabulation of data from hypervelocity impact experiments: U.S. Geol. Survey Astrogeologic Studies Semiannual Progress Report, Feb. 25, 1961--Aug. 24, 1961, p. 106-112.

Palmer, E. P., Grow, R. W., Johnson, D. K., and Turner, G. H. 1960, Cratering, experiment and theory: APGC-TR-60-39 (1), 4th Hypervelocity Impact Symposium, Eglin Air Force Base, Florida, Paper 13. p. 1-17.

Rice, M. H., McQueen, R. G., and Walsh, J. M., 1958, Compression of solids by strong shock waves: Solid State Physics, v. 6, p. 1-63.

Robertson, E. C., 1955, Experimental study of the strength of rocks: Geol. Soc. America Bull., v. 66, p. 1275-1314.

Summers, J. L., 1959, Investigation of high speed impact: regions of impact and impact at oblique angles: U.S. Natl. Aeronautics and Space Adm. Tech. Note D-94, 18 p.